

Features of Carbide Precipitation During Tempering of 15H2NMFA and 26HN3M2FA Steels

S.V. Belikov, V.A. Dub, P.A. Kozlov, A.A. Popov, A.O. Rodin, A.Yu. Churyumov and I.A. Shepkin

Abstract Thermodynamic calculation of the equilibrium phase composition and evolution of the size and composition of carbide particles was carried out using Thermo-Calc and TC-Prisma 2.0 in order to identify the optimal modes of the final heat treatment for 15H2NMFA and 26HN3M2FA steels. The formation of structure and mechanical properties complex of the investigated steels was experimentally studied after tempering. The model describing the precipitation and growth of carbide particles was suggested based on the experimental results. This model will be used as part of the developed control complex of thermodynamic and kinetic conditions for the formation of micro grains and nano-sized hardening phases.

Keywords Tempering · Carbides · Thermo-Calc · Sem

S.V. Belikov (✉) · A.A. Popov
Ural Federal University, Ekaterinburg, Russia
e-mail: s.v.belikov@urfu.ru

A.A. Popov
e-mail: a.a.popov@urfu.ru

V.A. Dub · A.O. Rodin · A.Yu. Churyumov
NUST MISiS, Moscow, Russia
e-mail: rodin@misis.ru

A.Yu. Churyumov
e-mail: churyumov@misis.ru

P.A. Kozlov · I.A. Shepkin
RF State Research Centre JSC “RPA “CNIITMASH”, Moscow, Russia
e-mail: paul.kozlov@gmail.com

I.A. Shepkin
e-mail: shtepkin@mail.ru

© The Author(s) 2018

K.V. Anisimov et al. (eds.), *Proceedings of the Scientific-Practical Conference “Research and Development - 2016”*, https://doi.org/10.1007/978-3-319-62870-7_48

The aim of the present study is to improve the performance of responsible parts of power engineering made from alloyed structural steels such as 15H2NMFA (increasing of the yield strength at 350 °C is not less than 10% compared to the specifications 0893-013-00212179-2003: not less than 440 MPa; reduction of a brittle-ductile transition temperature to -55 °C); and 20–30CrNiMoV (reduction of differences in the properties of the center and the periphery of the drum forging $\varnothing > 900$ mm at least to 20%). Science-based correction of metal products manufacturing technology with a large mass on the basis of thermodynamic and kinetic conditions control for the formation of micro grains and nano-sized hardening phases should provide a reduction of production costs (reduction of the total time of the manufacturing cycle up to 20%, including the heat treatment up to 30%; reduction of charge materials weight characteristic up to 10...15% (relative) as a result of optimization of an alloying elements content). The physical and mathematical model used for technology optimization should allow calculating the phase composition of selected steels, microstructure evolution, and grain size depending on the parameters of technological influences. The work was carried out by a consortium consisting of Ural Federal University, Ekaterinburg, NUST “MISiS” and JSC RPA CNIITMASH, Moscow, an industrial partner of the project—JSC “OMZ-Special Steels”, St. Petersburg.

At the first stage of the present work advanced compositions of steels were selected and quantitative estimation of the steels phase composition of Fe–Cr–Ni–Mo–V–Mn–Si–C system in the temperature range of 400–1600 °C was made by method of numerical thermodynamic simulation. Table 1 shows the chemical composition of investigated steels.

The software for thermodynamic simulation Thermo-Calc (TCW 5.0) with a database of steels thermodynamic properties TCFE6.0 was used for the tests mentioned above.

The input data for the calculation in the Thermo-Calc:

- The chemical composition of the simulated steels (11 compositions with average values of alloying elements in the range of grade and with the content of ferrite and austenite forming elements located at the top or bottom of the grade composition);

Table 1 The chemical composition of investigated steels

Steel grade	Weight content of chemical elements (%)						
	C	Si	Mn	Cr	Ni	Mo	
15H2NMFA-A	0.15– 0.18	0.15– 0.25	0.30– 0.60	1.8– 2.3	1.30– 1.50	0.5– 0.7	V 0.10–0.12 $S \leq 0.004$ $P \leq 0.004$ $As \leq 0.010$ $Cu \leq 0.10$ $Co \leq 0.03$
26HN3M2FA	0.22– 0.36	≤ 0.3	≤ 0.4	2.4– 3.8	3.4– 3.8	0.2– 0.7	V 0.05–0.15 $S \leq 0.01$ $P \leq 0.01$

- The test temperature range of 400–1600 °C;
- The pressure of 101325 Pa;
- Amount of substance in a system –1 mol.

Calculations have shown that at tempering range from 600 to 700 °C 15H2NMFA-A steel has a heterophase structure: special carbides such as M_7C_3 and $M_{23}C_6$ as well as a minor amount of carbides of MC-type based on vanadium and molybdenum were observed in addition to the basic ferrite matrix (Fig. 1a). The total content of the carbides at a temperature of 600 °C is 2.97%. Moreover, the complete dissolution of these phases occurs above temperatures of 800–840 °C. Modifying of the alloying elements content within grade composition do not lead to the changing of secondary phases type and their volume fraction ranges in a narrow range from 2.52 to 3.08%. The calculated values of the critical points A_1 and A_3 were found to be 707–741 °C and 794–808 °C respectively.

The 26HN3M2FA steel contains greater number of austenite-promoting elements (nickel, carbon black) than 15H2NMFA steel, which leads to increased austenite stability and expansion of austenite field: the temperature A_3 was found to be in a range from 725 to 772 °C. Moreover, a complete decomposition of austenite was observed in steels with a minimum content of γ -stabilizing elements (nickel, carbon, manganese). In this case, the temperature A_1 ranged from 623 to 664 °C.

The content of carbides (special carbides of M_7C_3 type and $M_{23}C_6$, and a minor amount of MC carbides based on vanadium and molybdenum Fig. 1b) is in a wider range than that of 15H2NMFA steel: in a range of 2.67–3.56%.

Thus, for the composition corresponding to the content of alloying elements on the upper limit (for grade), the presence of austenite is also possible (up to 4% at a tempering temperature –600 °C).

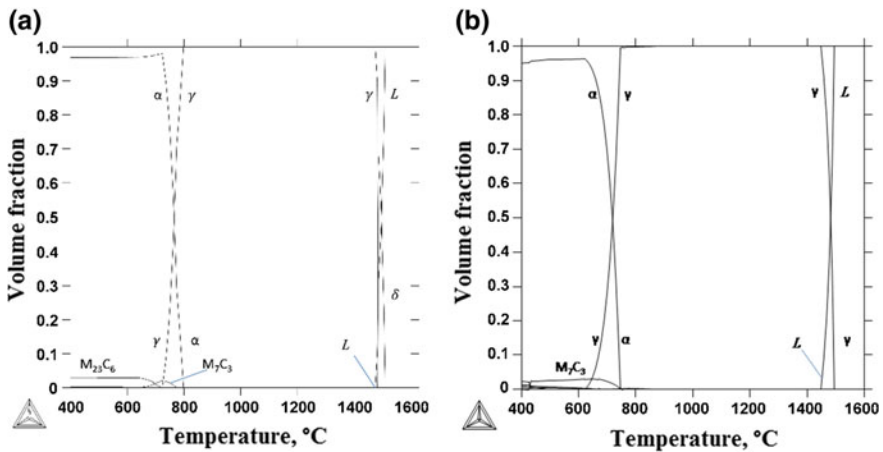


Fig. 1 The effect of temperature on the phase composition of steels **a** 15H2NMFA; **b** 26HN3M2FA

A volume fraction and a size of carbide particles which are formed as a result of the final heat treatment has a major influence on the precipitation hardening of investigated steels. Programs like DICTRA, PrecipiCalc, MatCalc, PanPrecipitation and TC-Prisma received a wide dissemination in the field of kinetics of the phase formation and growth in multicomponent systems (steels and alloys).

A common feature of the mentioned above software is the use of CALPHAD approaches as a basis for determination of the driving forces for the formation and growth of phase particles, the chemical potentials and diffusion mobility of system components [1].

For calculations of the growth kinetics of carbides, the following phases are considered:

- $M_{23}C_6$ and MC carbides in the ferrite matrix of 15H2NMFA steel at a temperature of 650 °C;
- $M_{23}C_6$, M_7C_3 and MC carbides in a ferritic matrix of 26HN3M2FA steel at a temperature of 600 °C.

Simultaneously, during the calculations the following assumptions were used:

- the precipitation and growth of carbides takes place in the body of the grain (i.e., diffusion in the volume of grain is controlling process of the phase precipitation and growth);
- calculations of precipitation and growth kinetics are carried out under isothermal conditions (i.e., for maximum constant tempering temperature), without taking into account the prehistory of heating and cooling for quenching and tempering;
- phase precipitations have an equiaxed shape and close to the stoichiometric composition or correspond it.

Furthermore, the definition of the interface energy is a requirement for the calculation of precipitation and growth kinetics of carbides: based on an analysis of literature data [1–3] for 15H2NMFA and 26HN3M2FA steels the value of the interface energy was assumed to be:

- for carbides $M_{23}C_6$ - $\gamma^{M_{23}C_6/\alpha} = 0.27\text{--}0.29 \text{ J/m}^2$;
- for carbides M_7C_3 - $\gamma^{M_7C_3/\alpha} = 0.41 \text{ J/m}^2$;
- for carbides MC - $\gamma^{VC/\alpha} = 0.56 \text{ J/m}^2$ and $\gamma^{(Mo,V)C/\alpha} = 0.36 \text{ J/m}^2$.

All calculations were carried out using TC-Prisma 2.0 program with thermodynamic and kinetic database of the materials properties TCFE7.0 and MOB2.0, respectively. Calculation shows that the volume fraction of the carbides increases with the passage of time and tends to asymptotes corresponding to the equilibrium phase content in the steel. It should be noted that exposure for about 90 h at 650 °C is sufficient for complete precipitation of $M_{23}C_6$ carbides ($\sim 3.3\%$), while the vanadium carbide precipitation does not occur completely (Fig. 2a).

Figure 2b shows the changes in size of $M_{23}C_6$ and MC carbide precipitates. The kinetics of changes in precipitates size is parabolic. A size of $M_{23}C_6$ carbides

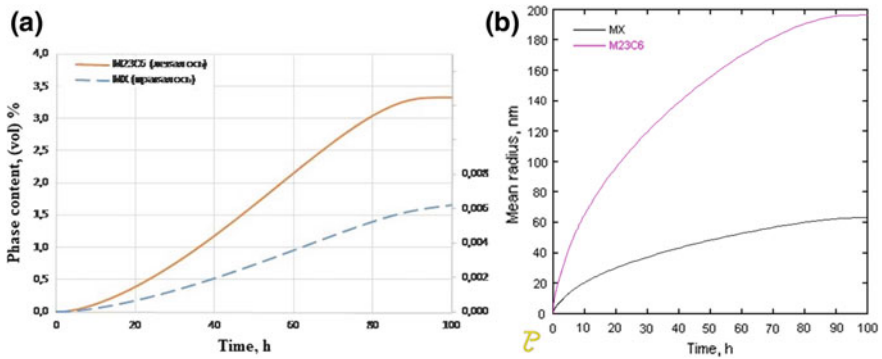


Fig. 2 Changing of carbides content (a) and the kinetics of their growth (b) for 15H2NMFA steel during isothermal aging for 100 h at a temperature of 650 °C

reaches about 195 nm (after 100 h) while a size of vanadium carbides reaches 62–65 nm.

Calculation made for 26HN3MFA steel shows that processes of carbides precipitation do not proceed completely at a given temperature and exposure time: the curves do not indicate a transition to a process of “saturation” (Fig. 3a).

It should be noted that the values obtained for the phases in the steel does not correspond to the values obtained as a result of thermodynamic equilibrium calculations: according to the calculations of the kinetics of phase precipitation, the main phase is the molybdenum MC-type carbide, whereas the calculations made in the Thermo-Calc program indicate that the main secondary phase in this steel is a carbide such as M_7C_3 . This deviation may be related to a necessity to clarify the initial conditions of the settlement—the interphase energy. Due to a lack of information about the value of $\gamma_{600^\circ\text{C}}^{M23C6/\alpha}$, $\gamma_{600^\circ\text{C}}^{M7C3/\alpha}$ and $\gamma_{600^\circ\text{C}}^{MC/\alpha}$ the experimental studies for subsequent calibration of the model is required for the investigated steels at a given temperature.

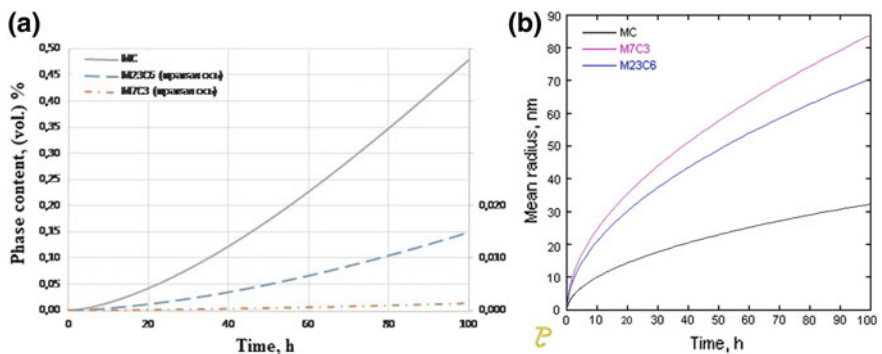


Fig. 3 Changing of carbides content (a) and the kinetics of their growth (b) in 26HN3M2FA steel during isothermal aging for 100 h at a temperature of 600 °C

The kinetic curves of carbides size are parabolic as well as in the case of 15H2NMFA steel. According to the calculations the carbides M_7C_3 and $M_{23}C_6$ have the greatest size. The carbide sizes after isothermal exposure for 100 h at 600 °C value from 70 up to 85 nm, while the size of MC-type carbides is 30–35 nm.

Laboratory melting steels were studied at the second stage of research.

Melting and casting of laboratory ingots were produced at the experimental basis of JSC RPA CNIITMASH. Melting was carried out in an induction furnace with a basic magnesite lining of 50 kg capacity crucible, by melting the charge material. Pure or highly purified charge materials were used for the production of laboratory ingots of hull and rotor steels.

The feeding of materials into the open induction furnace was carried out in the following order: armco iron, metallic chromium, nickel, synthetic iron. The ferrosilicon for pre-deoxidation was added during melting. Slag mixture from lime, fluorspar and aluminum powder was partly added during melting. Molybdenum was introduced during the process of the liquid bath appearance. Ferrovandium was introduced in the liquid melt. Ferrosilicon and manganese were introduced into the furnace behind 3–5 min to release. Aluminum was added before the release, then a temperature measurement was carried out. The metal temperature was estimated to be 1610 °C.

The metal was tapped from the furnace to 4 ingots with a mass of 12 kg each. After an ingots casting, the exothermal mixture was introduced to the metal surface in an amount of 100 g per an ingot. Ladle samples were selected to carry out the chemical analysis, the results of which are presented in Tables 2 and 3.

Ingots were cold before forging. Heating of ingots in an electric furnace was performed under the regime: furnace loading at 700 °C, heating up to 1190 °C (speed of a furnace temperature rising –130 °C/h), 60 min exposure at 1190 °C. Heating time was about 5 h.

Interim heating of forgings was performed up to 1180 °C. Heating of forgings from the temperature of forging closing (~850–900 °C) was performed in the same furnace, heated to 1180 °C. Final deformation temperature, including cutting operation was not lower than 850 °C.

The investigated steels have shown a sufficient technological plasticity. However, the defects as fine cracks were formed in several bars after the last removal from furnace. Figure 4 shows the martensitic-bainitic microstructure of investigated steels. An insignificant amount of vanadium carbide with a size of 30–50 nm was observed in the structure. Table 4 shows the heat treatment modes.

The effect of heat treatment parameters was considered by an example of 15H2NMFA steel.

Tempering for 2 h leads to the precipitation of special carbides particles on the boundaries of the former martensite laths (Fig. 5a). The obtained properties complex: $\sigma_{0.2} = 820$ MPa; $\sigma_b = 925$ MPa; $\delta = 17.5\%$; $\psi = 64\%$. Increasing of exposure time to 4 h leads to the additional precipitation of carbides dispersed particles of another type (Fig. 5b) and a certain increase in tensile strength ($\sigma_{0.2} = 850$ MPa; $\sigma_b = 955$ MPa) while keeping high ductility ($\delta = 17\%$; $\psi = 65\%$). A further

Table 2 The specified and the actual chemical composition of 15H2NMFA-A ingots

Melting	Weight content of chemical elements (%)												
	C	Si	Mn	Cr	Mo	Ni	P	S	V	As	Cu	Co	
68	0.15	0.23	0.53	2.11	0.63	1.42	0.002	0.003	0.11	<0.01	<0.01	<0.01	
125	0.16	0.23	0.54	2.28	0.63	1.44	0.002	0.003	0.11	<0.01	0.01	0.01	
Standard	0.15–0.18	0.15–0.25	0.45–0.6	2.1–2.3	0.6–0.7	1.35–1.5	<0.004	<0.004	0.1–0.12	<0.01	<0.03	<0.03	

Table 3 The specified and the actual chemical composition of 26HN3M2FA ingots

Melting	Weight content of chemical elements (%)										
	C	Si	Mn	Cr	Mo	Ni	P	S	V	Al	Cu
79	0.28	0.03	0.45	1.69	0.61	3.71	0.002	0.003	0.16	0.02	
111	0.29	0.04	0.51	1.70	0.58	3.71	0.003	0.004	0.16	0.05	0.03
Standard	0.25–0.30	<0.04	0.3–0.6	1.3–1.7	0.5–0.7	3.4–3.8	<0.01	<0.012	0.12–0.18		<0.2

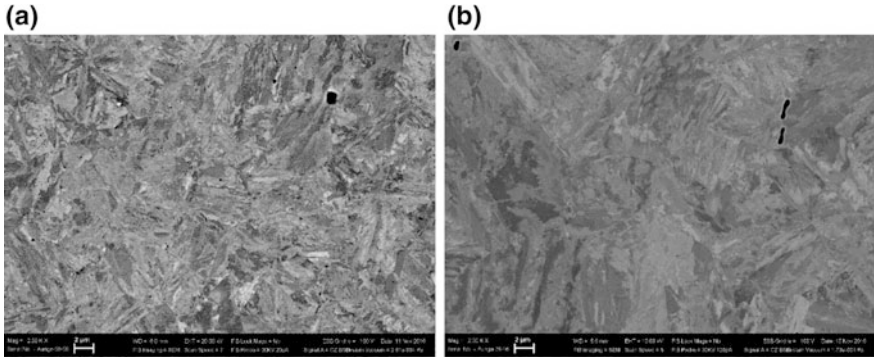


Fig. 4 SEM images showing the initial structure of forged steels **a** 15H2NMFA; **b** 26HN3M2FA

Table 4 Modes of heat treatment of forged bars made from 15H2NMF and 20–30CrNiMoV steels

Steel	Melting	Heat treatment mode		
15H2NMF	68	Preparation of samples for investigation of the grain structure evolution using Gleeble System 3800		
		Fine grain	Average grain	Oversize grain
		900 °C (exposure for 1, 2 and 3 h. respectively)	1050 °C (exposure for 1, 2 and 3 h. respectively)	1250 °C (exposure for 1, 2 and 3 h. respectively)
	125	Preparation of samples for creating of the heat treatment model: Quenching from 910–920 °C (after exposure for 3 h) with rapid cooling. Tempering at 650 °C for 2–4–8–16–32–62 h.		
26HN3M2FA	79	Preparation of samples for investigation of the grain structure evolution using Gleeble System 3800		
		Fine grain	Average grain	Oversize grain
		900 °C (exposure for 1, 2 and 3 h. respectively)	1050 °C (exposure for 1, 2 and 3 h. respectively)	1250 °C (exposure for 1, 2 and 3 h. respectively)
	111	Preparation of samples for creating of the heat treatment model: Quenching from 840–860 °C (after exposure for 3 h) with cooling rate (100–200 °C/h). Tempering at 650 °C for 2–4–8–16–32–62 h		

increase in exposure time leads to a weakening associated with the process of coalescence. After 62 h exposure strength reduces to $\sigma_{0.2} = 600$ MPa; $\sigma_b = 715$ MPa, while ductility increases insignificantly: $\delta = 22\%$; $\psi = 71\%$. This fact is connected with the coarsening of carbides precipitated on the boundaries laths (Fig. 5c). A similar dependence is observed for 26HN3M2FA steel, however a slight increase in strength is observed after exposure for 16 h.

The experimental results are in good agreement with the calculated, however, the secondary hardening is not predicted.

The calculation of the average rate of nucleus formation with a critical size shows that this is not a controlling factor for the process. However, the calculation indicates sensitivity to the value of ΔG (the Gibbs energy) and explains why the primary growth always occurs at the grain boundaries and dislocations.

The calculation of the grain boundaries energy increases the nucleation rate by 4 orders. A consideration of the dislocations presence shows that particles can appear earlier practically at all dislocations.

Particle growth is described by the following equation in case if they are isolated from each other, i.e., due to the diffusion supply of substance (Particles in a volume of grain with the average distance corresponding to a specified density of dislocations):

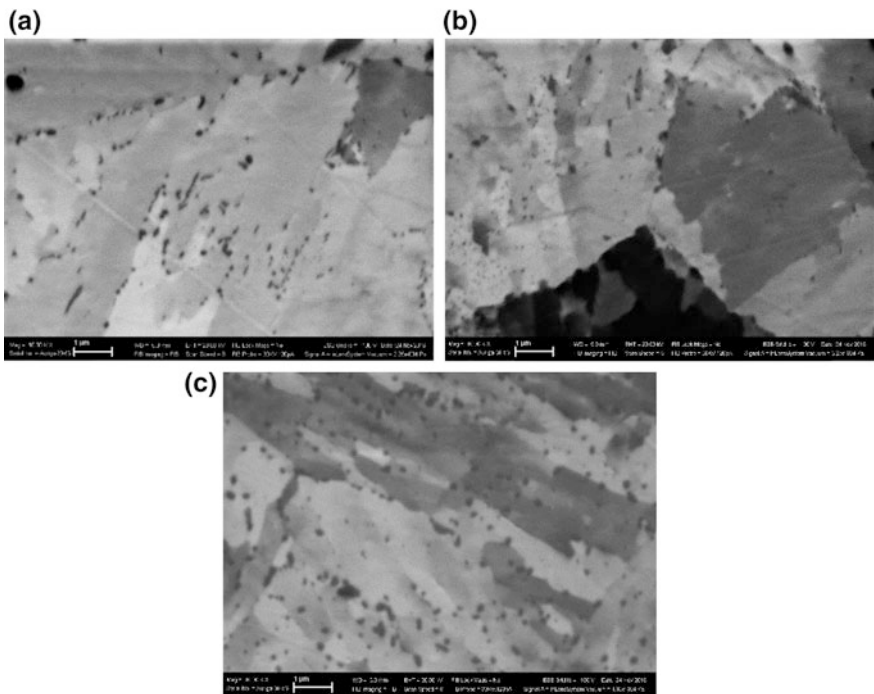


Fig. 5 SEM images showing the microstructure of the 15H2NMFA steel after quenching and tempering at a temperature of 650 °C: **a** 2 h; **b** 4 h; **c** 62 h

$$c(r, t) = c_0 + (c_1 - c_0) \times \frac{\varphi_j\left(r/(Dt)^{1/2}\right)}{\varphi_j\left(R/(Dt)^{1/2}\right)}, \tag{1}$$

where, function

$$\varphi_j(\xi) = \int_x^\infty \xi^{1-j} \exp(-\xi^2/4) d\xi \tag{2}$$

If temperature process assumed to be constant in the volume, then D (diffusion coefficient) is constant, and $j = 3$.

Calculation of particle size in the grain boundaries, taking into account the “absorption” of some by other particles. According to the developed model the particle size can be calculated as:

$$r = \sqrt[4]{\frac{4\gamma\Omega C\delta D_{g,b}t}{3ABkT}}, \tag{3}$$

where γ —interfacial tension; C —the equilibrium concentration of the substance in the border; $D_{g,b}$ —Grain boundary diffusion coefficient; k —Boltzmann’s constant; δ —the width of the grain boundary; $A = \frac{2}{3} - \frac{\gamma_{g,b}}{2\gamma} + \frac{1}{3} \left(\frac{\gamma_{g,b}}{2\gamma}\right)^3$ —geometrical constant; $B = \frac{1}{2} \ln\left(\frac{r}{f}\right)$ —morphological constant; T —temperature; r —the radius; t —time; Ω —the atomic volume (Fig. 6).

It can be seen that the obtained values are around 200 nm for 100 h, and extremely sensitive to temperature exposure, while exposure time in the latter stages has almost no effect.

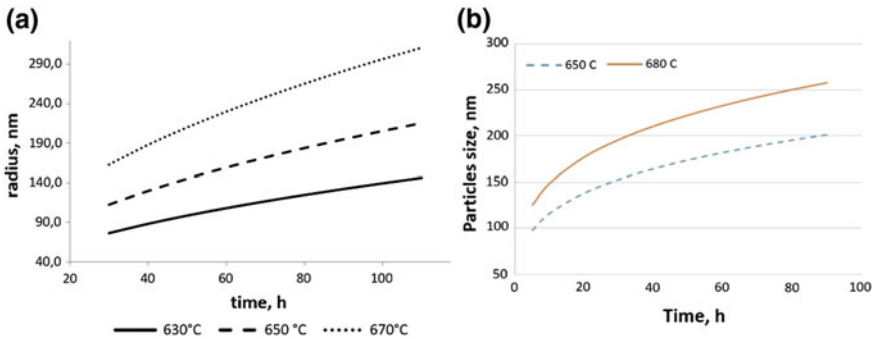


Fig. 6 Calculated size of particles (a) in the volume of grain; (b) at grain boundaries

Conclusions

The values of the volume fraction and size of carbide particles which were formed as a result of tempering were calculated using Thermo-Calc and TC-Prisma 2.0 programs. These values allow to predict the main tendencies and relatively roughly estimate the temperature and time parameters of the final heat treatment modes. However, the inability to adjust the simulation models incorporated in commercial products, provides an opportunity to improve the superiority of the developed national control complex of thermodynamic and kinetic conditions for the formation of micro-sized and nano-sized hardening phases. The features of carbide precipitation were experimentally studied. The conditions for obtaining the specified properties of 15H2NMFA and 26HN3M2FA steels after tempering were established.

Acknowledgements Research are carried out (conducted) with the financial support of the state represented by the Ministry of Education and Science of the Russian Federation.

Agreement (contract) no 14.578.21.0114 27.10.2015.

Unique project Identifier: RFMEFI57815X0114.

References

1. Kozeschnik, E.: Modeling Solid-state Precipitation. Momentum Press, New York, (2013), 464 p
2. Hou, Z.Y., Hedstrom, P., Xu, Y.B., Wu, D., Odqvist, J.: Microstructure of martensite in Fe–C–Cr and its implications for modelling of carbide precipitation during tempering. *ISIJ Int.* **54** (11), 2649–2656 (2014)
3. Prat, O., Garcia, J., Rojas, D., Sanhueza, J.P., Camurri, C.: Study of nucleation, growth and coarsening of precipitates in a novel 9%Cr heat resistant steel: experimental and modeling. *Mater. Chem. Phys.* **143**(2), 754–764 (2014)

Open Access This chapter is licensed under the terms of the Creative Commons Attribution 4.0 International License (<http://creativecommons.org/licenses/by/4.0/>), which permits use, sharing, adaptation, distribution and reproduction in any medium or format, as long as you give appropriate credit to the original author(s) and the source, provide a link to the Creative Commons license and indicate if changes were made.

The images or other third party material in this chapter are included in the chapter's Creative Commons license, unless indicated otherwise in a credit line to the material. If material is not included in the chapter's Creative Commons license and your intended use is not permitted by statutory regulation or exceeds the permitted use, you will need to obtain permission directly from the copyright holder.

